



Optical investigations of the normal and superconducting states reveal two electronic subsystems in iron pnictides

D. Wu,^{1,*} N. Barišić,^{1,†} P. Kallina,¹ A. Faridian,¹ B. Gorshunov,¹ N. Drichko,¹ L. J. Li,² X. Lin,² G. H. Cao,² Z. A. Xu,² N. L. Wang,³ and M. Dressel¹

¹*Physikalisches Institut, Universität Stuttgart, Pfaffenwaldring 57, 70550 Stuttgart, Germany*

²*Department of Physics, Zhejiang University, Hangzhou 310027, People's Republic of China*

³*Institute of Physics, Chinese Academy of Sciences, Beijing 100190, People's Republic of China*

(Received 22 February 2010; published 25 March 2010)

Infrared reflectivity measurements on several 122 iron pnictides reveal the existence of two electronic subsystems. The one gapped due to the spin-density-wave transition in the parent materials, such as EuFe_2As_2 , is responsible for superconductivity in the doped compounds, such as $\text{Ba}(\text{Fe}_{0.92}\text{Co}_{0.08})_2\text{As}_2$ and $\text{Ba}(\text{Fe}_{0.95}\text{Ni}_{0.05})_2\text{As}_2$. Analyzing the dc resistivity and scattering rate of this contribution, a hidden T^2 dependence is found in the normal state. The second subsystem gives rise to incoherent background, present in all 122 compounds, which is basically temperature independent but affected by the superconducting transition.

DOI: [10.1103/PhysRevB.81.100512](https://doi.org/10.1103/PhysRevB.81.100512)

PACS number(s): 74.25.Gz, 74.25.Jb, 75.30.Fv

In the course of the past year, it became apparent that both the normal and superconducting states of iron pnictides are more complex than in conventional metals.^{1,2} Understanding their magnetic and structural orders in parallel to superconductivity is one of the main challenges. An additional complication is the presence of several bands close to the Fermi energy where nesting might be crucial for the magnetic order.^{3,4} Substituting Ba by K in BaFe_2As_2 , for instance, introduces holes and affects structural and spin-density-wave (SDW) transitions, which are both suppressed for the benefit of superconductivity.⁵ When Co or Ni partially replaces Fe also both transitions are suppressed and superconductivity is observed up to $T_c=25$ K.^{6,7} The proximity of a magnetic ground state raises the question about the role of magnetic fluctuations,⁸ which—together with the observed anomalous transport behavior—evokes a quantum-phase-transition scenario for superconductivity.^{9,10} Here we compare the optical properties on different 122-iron pnictide compounds and find that the low-frequency conductivity spectra can be decomposed into a broad temperature-independent part and a narrow contribution around zero frequency. The latter is the only contribution which depends considerably on temperature. By the closer analysis of this contribution a T^2 in dc resistivity and scattering rate is revealed in the normal state.

Single crystals of EuFe_2As_2 , $\text{Ba}(\text{Fe}_{0.92}\text{Co}_{0.08})_2\text{As}_2$, and $\text{Ba}(\text{Fe}_{0.95}\text{Ni}_{0.05})_2\text{As}_2$ were grown using FeAs as self-flux dopants^{7,9} and characterized by x-ray, EDX-microanalysis, transport, and susceptibility measurements [Figs. 3(a) and 3(b)]. The high reproducibility of the resistivity measurements and the sharp transition observed in the susceptibility indicate that the samples are homogeneously doped.¹¹ The temperature-dependent optical reflectivity (in *ab* plane) was measured in a wide frequency range from 20 to 37 000 cm^{-1} using a series of spectrometers. The low-frequency extrapolation was done according to the dc conductivity measured on the same crystals. The complex optical conductivity $\hat{\sigma}(\omega)=\sigma_1(\omega)+i\sigma_2(\omega)$ was calculated from the reflectivity spectra using Kramers-Kronig analysis.

In Fig. 1 we present the in-plane optical properties of $\text{Ba}(\text{Fe}_{0.92}\text{Co}_{0.08})_2\text{As}_2$ and $\text{Ba}(\text{Fe}_{0.95}\text{Ni}_{0.05})_2\text{As}_2$ at different temperatures. The reflectivity is metallic but does not exhibit

a clear-cut plasma edge similar to other 122 iron pnictide compounds.^{12–19} The optical conductivity contains a broad double peak in the midinfrared and near-infrared that does not change considerably with temperature. As T decreases, a Drude-like contribution develops and becomes narrower. Both features are separated by a minimum in $\sigma_1(\omega)$ around 1000 cm^{-1} .

When we try to fit the normal-state spectra by a minimum number of Drude and Lorentz contributions,²⁰ we obtain a

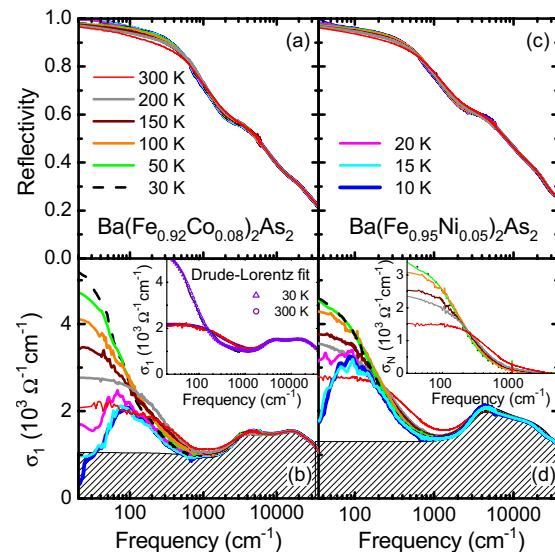


FIG. 1. (Color online) Optical reflectivity and conductivity of $\text{Ba}(\text{Fe}_{0.92}\text{Co}_{0.08})_2\text{As}_2$ and $\text{Ba}(\text{Fe}_{0.95}\text{Ni}_{0.05})_2\text{As}_2$ measured at different temperatures between 10 and 300 K in a wide spectral range. In the normal state the optical conductivity can be separated in temperature dependent and independent parts. The temperature independent part, indicated by the densely hatched area, consists from the incoherent broad term σ_B and effective oscillators at higher frequencies. The unshaded area below the curves is temperature dependent and can be described by a single Drude term (σ_N) as discussed in the text. Quality of Drude-Lorentz fits is demonstrated in the inset of panel (b) for two temperatures $T=30$ and 300 K. Temperature evolution of σ_N in the normal state of the Ni-compound is shown in the inset of panel (d).

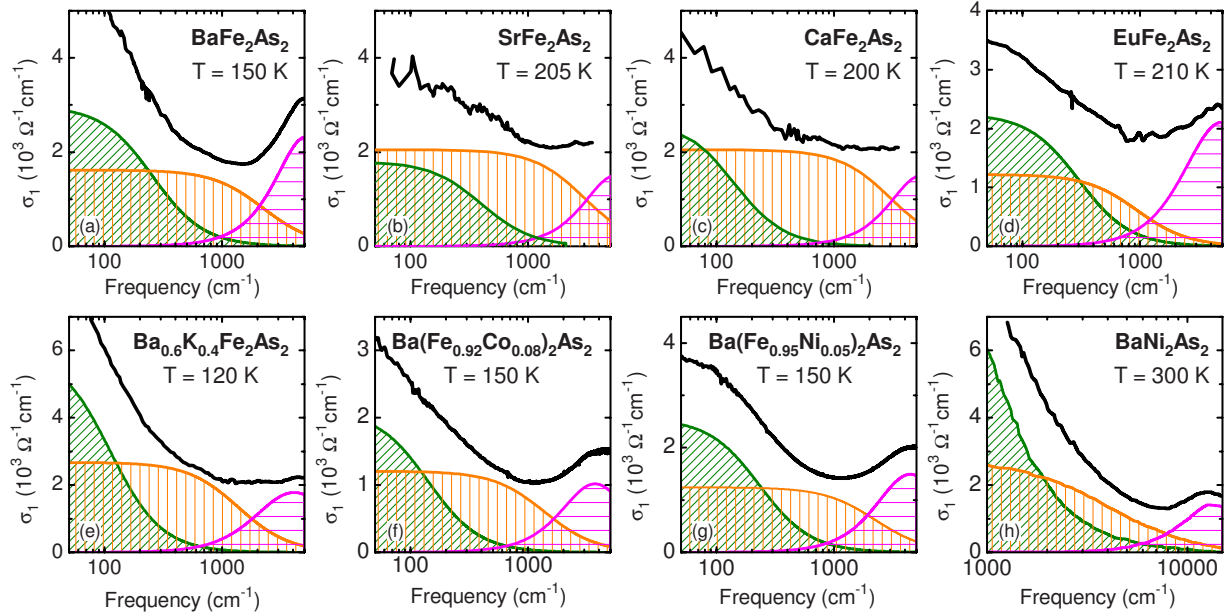


FIG. 2. (Color online) Comparison of the optical conductivity of different iron pnictides, in the normal state, indicates that the decomposition in two Drude terms (σ_N and σ_B shaded densely green and medium orange, respectively) plus oscillators in the midinfrared (e.g., one of them is indicated by sparsely hatched magenta) holds for the whole 122 family. The spectra of the parent compounds at temperatures above the SDW transition: (a) BaFe_2As_2 (Ref. 12), (b) SrFe_2As_2 (Ref. 12), (c) CaFe_2As_2 (Ref. 13), and (d) EuFe_2As_2 (Ref. 14). For $T > T_c$ the conductivity spectra of the electron doped superconductor $\text{Ba}_{0.6}\text{K}_{0.4}\text{Fe}_2\text{As}_2$ (Ref. 15), the hole doped superconductors (f) $\text{Ba}(\text{Fe}_{0.92}\text{Co}_{0.08})_2\text{As}_2$ and (g) $\text{Ba}(\text{Fe}_{0.95}\text{Ni}_{0.05})_2\text{As}_2$ are very similar. (h) When Fe is completely substituted by Ni, the material is more metallic, but the room-temperature spectrum of BaNi_2As_2 (Ref. 16) can be decomposed in the same way with a larger spectral weight of the Drude components.

satisfactory description only by using two Drude terms.²¹ Interestingly, this decomposition holds universally for all temperatures, as shown in Fig. 1, and for eight different 122 iron pnictides indicating that it might be universal for the whole family. This is illustrated in Fig. 2 where the optical conductivity is displayed in a large frequency range for parent compounds $X\text{Fe}_2\text{As}_2$ ($X=\text{Ba},\text{Sr},\text{Ca},\text{Eu}$), as well as for hole-doped $\text{Ba}_{0.6}\text{K}_{0.4}\text{Fe}_2\text{As}_2$ and for the completely substituted BaNi_2As_2 .^{12–16} Simple oscillators (two are sufficient) model the midinfrared properties adequately well. A broad contribution σ_B mimics the considerable background conductivity that seems to be similar for all compounds and does not change appreciably with temperature. As will be discussed later, the distinct properties of the particular material are solely determined by the second Drude term σ_N with a width of approximately 100 cm^{-1} in the case of $\text{Ba}(\text{Fe}_{0.92}\text{Co}_{0.08})_2\text{As}_2$. Its spectral weight is smaller by a factor of 3–5 compared to σ_B . Upon cooling, the spectral weight is roughly conserved for each of these two fractions, i.e., there is no transfer between these two subsystems. Our finding is in accord with angle-resolved photoemission (ARPES) data²² which indicate that the multiband structure does not change considerably upon doping and temperature.

In order to analyze the temperature dependence of σ_N at $\omega=0$, we have measured the dc resistivity [see Fig. 3(a)], then simply deduce a constant σ_B from the graphs displayed in Fig. 2 and consider $\sigma_N(T)=\sigma_{\text{total}}(T)-\sigma_B$. The result is surprising but very simple, namely, $\rho_N=1/\sigma_N \propto T^2$ over the broad temperature range, as shown in Fig. 3(c). Importantly, an independent confirmation of this finding is obtained di-

rectly from the decomposition of the low-frequency conductivity of $\text{Ba}(\text{Fe}_{1-x}\text{M}_x)_2\text{As}_2$. The Drude fit $\sigma_N(\omega)=\sigma_N(\omega=0)/(1+\omega^2\tau_N^2)$ yields a scattering rate $1/\tau_N(T) \propto T^2$ as well [Fig. 3(d)]. These results evidence a deep physical consistency of our decomposition.

We want to point out that due to the broad frequency range covered by only two Drude contributions, the fits are robust and give well-defined parameters σ_B , $\sigma_N(T)$, and $1/\tau_N(T)$. Furthermore, we restrain ourselves by assuming σ_B basically as temperature independent; and since the dc conductivity is determined separately, that leaves only $1/\tau_N(T)$ as a fit parameter. Moreover, as a result of such fit procedure it turns out that the coherent Drude term preserves its spectral weight within an uncertainty of 2%.

It is of interest to compare our findings with the Hall-effect study on the series $\text{Ba}(\text{Fe}_{1-x}\text{Co}_x)_2\text{As}_2$ (Ref. 23) which also reveals the same T^2 temperature dependence of the scattering rate. Those authors attributed it to the Fermi liquid. Furthermore, other iron pnictides behave in a very similar way, as demonstrated on $\text{Ba}(\text{Fe}_{0.95}\text{Ni}_{0.05})_2\text{As}_2$ in Fig. 3(c), confirming that such behavior is quite general. Notably, a T^2 behavior of the resistivity is also found in 1111 compounds.^{24,25}

We note that our way to a hidden T^2 temperature dependence differs somewhat from previously reported findings. Those works analyzed the resistivity prior to its decomposition, having both contributions, $\sigma_N(T)$ and σ_B , mixed. The “anomalous” temperature dependence of the resistivity ($\rho_0 + AT^n$ or $\rho_0 + AT + BT^2$) and the proximity of the magnetic phase have been considered as an indication that the

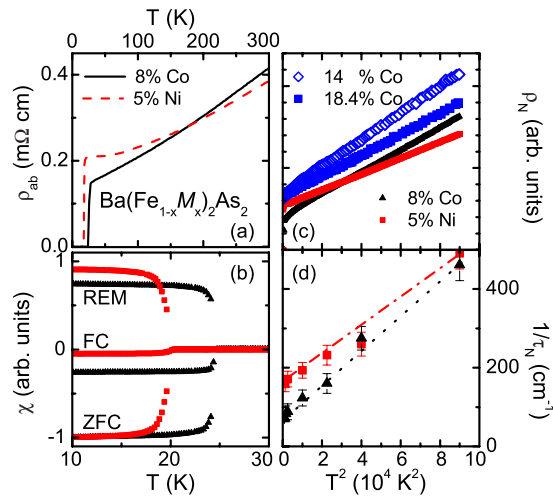


FIG. 3. (Color online) (a) Temperature dependence of the electrical resistivity of $\text{Ba}(\text{Fe}_{0.92}\text{Co}_{0.08})_2\text{As}_2$ and $\text{Ba}(\text{Fe}_{0.95}\text{Ni}_{0.05})_2\text{As}_2$ crystals. (b) The field-cooled (FC), zero-field-cooled (ZFC), and remanent (REM) susceptibility exhibit a sharp change at the transition temperature ($T_c=25$ and 20 K). (c) “Narrow Drude” contribution to dc resistivity plotted as a function of T^2 , as obtained by decomposition $\rho_N(T)=[\sigma_{\text{total}}(T)-\sigma_B]^{-1}$, where the σ_B is constant in temperature. The data are presented in arbitrary units since $\text{Ba}(\text{Fe}_{0.86}\text{Co}_{0.14})_2\text{As}_2$ and $\text{Ba}(\text{Fe}_{0.816}\text{Co}_{0.184})_2\text{As}_2$ are taken from Ref. 9 where no absolute values are given. (d) Temperature dependence of the scattering rate $1/\tau_N(T)$ obtained from the fit of the low-frequency optical data by the Drude model.

superconducting ground state is a consequence of underlying quantum criticality.^{9,10,21} Indeed as shown in Fig. 3(a) the total resistivity is clearly not quadratic in temperature and can be well fitted with AT^n with $n=1.25$ for $\text{Ba}(\text{Fe}_{0.92}\text{Co}_{0.08})_2\text{As}_2$ and $n=1.5$ for $\text{Ba}(\text{Fe}_{0.95}\text{Ni}_{0.05})_2\text{As}_2$. Only when the incoherent part, determined by optical conductivity, is subtracted, the T^2 law appears in both samples, as demonstrated in Fig. 3(c). With doping the dc resistivity gets considerably smaller,^{23,26} because σ_N grows. Consequently the contribution of the incoherent term to σ_{total} becomes less important. This explains the change in the overall power-law coefficient upon doping,²⁶ eventually leading to $n=2$. Our decomposition of the optical conductivity and dc resistivity holds for all analyzed 122 iron pnictides and all measured temperatures, revealing the T^2 behavior in σ_N . This result is physically transparent²¹ and seems to be quite universal.

Next we analyze the superconducting state in detail. Upon passing the superconducting transition the reflectivity of $\text{Ba}(\text{Fe}_{0.92}\text{Co}_{0.08})_2\text{As}_2$ increases considerably below 70 cm^{-1} , as can be seen in Fig. 4(a); for $\text{Ba}(\text{Fe}_{0.95}\text{Ni}_{0.05})_2\text{As}_2$ a similar behavior is observed around 60 cm^{-1} . The way it approaches unity with a change in curvature causes a gaplike structure in the optical conductivity below 100 cm^{-1} [Fig. 4(b)]. The removal of spectral weight in $\sigma_1(\omega, T)$ compared to the normal state conductivity $\sigma^{(n)}(\omega, T \approx 30\text{ K})$ extends all the way up to approximately 150 cm^{-1} . From the missing area,²⁰ $A = \int [\sigma_1^{(n)}(\omega) - \sigma_1^{(s)}(\omega)] d\omega$ we estimate the penetration depth to $\lambda = c/\sqrt{8A} = (3500 \pm 350)\text{ \AA}$ and $(3000 \pm 300)\text{ \AA}$ for the Co and Ni compounds, respectively. Notably, both materials obey the universal scaling relation of the superfluid density

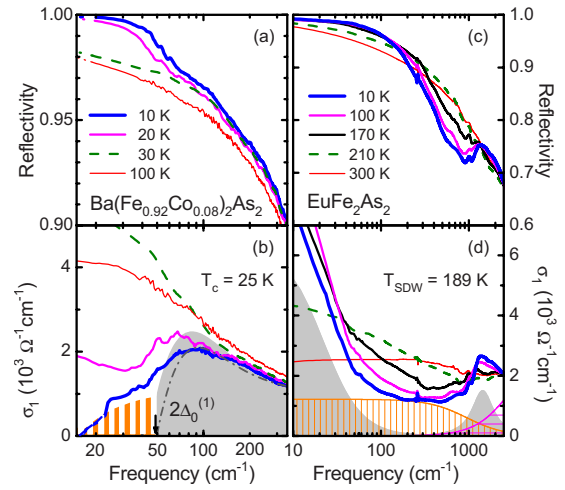


FIG. 4. (Color online) Reflectivity and conductivity of $\text{Ba}(\text{Fe}_{0.92}\text{Co}_{0.08})_2\text{As}_2$ and EuFe_2As_2 above and below the superconducting and SDW transitions. (a) The way the reflectivity of $\text{Ba}(\text{Fe}_{0.92}\text{Co}_{0.08})_2\text{As}_2$ approaches unity is indicative for the development of the superconducting gap. The dotted lines corresponds to the extrapolations. (b) The optical conductivity $\sigma_1(\omega, T)$ is gradually depleted up to approximately 150 cm^{-1} . The dash-dotted curve is calculated for the lowest temperature assuming one gap $2\Delta_0^{(1)} = 50\text{ cm}^{-1}$ and the shaded area by assuming gaps $2\Delta_0^{(1)} = 50\text{ cm}^{-1}$ in the $\sigma_N(\omega)$ component (mainly gray area) and $2\Delta_0^{(2)} = 17\text{ cm}^{-1}$ in the $\sigma_B(\omega)$ background (mainly orange area). [(c) and (d)] For $T < T_{\text{SDW}}$, a gap in the excitation spectrum of EuFe_2As_2 opens. Part of the spectral weight of σ_N shifts from low frequencies to above approximately 1000 cm^{-1} ; but a small Drude-like peak remains. The incoherent background $\sigma_B(\omega)$ remains basically temperature independent. The fit by the Drude-Lorentz model corresponds to $T=10\text{ K}$.

$\rho_s \propto A$ and the transition temperature T_c .^{27,28} This indicates that the main features of the superconducting state are well captured by the optical conductivity.

To get further insight, we model our spectra by the BCS theory for the frequency and temperature-dependent conductivity.²⁹ As seen by the dash-dotted lines in Fig. 4(b), a decent description is obtained with gap value of 50 cm^{-1} . Following the suggestions of two isotropic gaps, both opening simultaneously below T_c ,^{22,30,31} we obtain an even better description with $2\Delta_0^{(1)} = 50\text{ cm}^{-1}$ in the narrow Drude term only, and a second smaller gap $2\Delta_0^{(2)} = 17\text{ cm}^{-1}$ which affects the broad background.³² Similarly, the description of $\text{Ba}_{0.6}\text{K}_{0.4}\text{Fe}_2\text{As}_2$ suggests two superconducting gaps.¹⁸ This indicates that the hole-doped iron pnictides behave in the same way as the electron-doped compounds and that our conclusions are universal in this sense. The gap values obtained from our study are $2\Delta_0^{(1)}/k_B T_c = 2.5-3$, and 1 for the small gap. ARPES experiments on the K doped compound yield to higher gap values of $2\Delta_0^{(1)}/k_B T_c = 6.8$ and $2\Delta_0^{(2)}/k_B T_c < 3$.²² It is worthwhile to recall the situation of the two-gap superconductor MgB_2 , for which several methods evidence two gaps, while far-infrared measurements see only one. By now it is not understood why the optical results agree better with the smaller gap value although they should be sensitive only to the large one.³³ Due to the proximity of the superconductivity and magnetic ground state it is instruc-

tive to compare our results with those obtained on parent compounds. Upon passing through the SDW transition of EuFe_2As_2 , for instance,¹⁴ a gap in the excitation spectrum opens since parts of the Fermi surface are removed. Importantly, as demonstrated in Fig. 4(d), only spectral weight of σ_N shifts from low frequencies to above approximately 1000 cm^{-1} . The incoherent background σ_B remains basically unchanged. A small Drude-like peak (accounting for the metallic dc properties) remains and becomes very narrow as T is reduced. On the other hand, the metallic state of the $\text{Ba}(\text{Fe}_{1-x}\text{M}_x)_2\text{As}_2$ compounds ($M=\text{Co}$ or Ni , close to optimally doping) does not exhibit any trace of the SDW pseudogap (Fig. 1). Upon cooling down to the superconducting transition, $\sigma_N(\omega)$ gradually narrows and grows [Figs. 1(b) and 1(d)]. Importantly, at T_c a dominant superconducting gap develops in σ_N , i.e., it is associated with the same parts of the Fermi surface gaped by the SDW in parent compounds.

Our analysis of the optical conductivity in the normal and broken-symmetry ground states of iron pnictides reveals two sorts of conduction electrons associated with σ_B and σ_N (Fig. 2). The broad term σ_B is temperature independent. We ascribe it to an incoherent subsystem which seems to be a common fact in all iron pnictides. The narrow Drude-like contribution σ_N dominates the conduction in the pnictides. It reveals a T^2 behavior in the resistivity and scattering rate. Furthermore the dominant gap at $2\Delta^{(1)}$ in electron doped $\text{Ba}(\text{Fe}_{1-x}\text{M}_x)_2\text{As}_2$ and the SDW gap in parent compound EuFe_2As_2 develop in σ_N , which signifies that the underlying ground states of iron pnictides involve the same parts of the Fermi surface.

We acknowledge the help of J. Braun and E.S. Zhukova. D.W. and N.B. were supported by the Alexander von Humboldt Foundation. N.D. thanks the Magarete-von-Wrangell-Programm. This work was supported by the NSF of China.

*dan.wu@pi1.physik.uni-stuttgart.de

†barisic@pi1.physik.uni-stuttgart.de

¹M. R. Norman, *Physics* **1**, 21 (2008).

²K. Ishida, Y. Nakai, and H. Hosono, *J. Phys. Soc. Jpn.* **78**, 062001 (2009).

³J. Dong *et al.*, *Europhys. Lett.* **83**, 27006 (2008).

⁴D. J. Singh, *Phys. Rev. B* **78**, 094511 (2008).

⁵M. Rotter *et al.*, *New J. Phys.* **11**, 025014 (2009).

⁶A. S. Sefat, R. Jin, M. A. McGuire, B. C. Sales, D. J. Singh, and D. Mandrus, *Phys. Rev. Lett.* **101**, 117004 (2008).

⁷L. J. Li *et al.*, *New J. Phys.* **11**, 025008 (2009).

⁸F. L. Ning, K. Ahilan, T. Imai, A. S. Sefat, R. Jin, M. A. McGuire, B. C. Sales, and D. Mandrus, *J. Phys. Soc. Jpn.* **78**, 013711 (2009); *Phys. Rev. B* **79**, 140506(R) (2009).

⁹J.-H. Chu, J. G. Analytis, C. Kucharczyk, and I. R. Fisher, *Phys. Rev. B* **79**, 014506 (2009).

¹⁰M. Gooch, B. Lv, B. Lorenz, A. M. Guloy, and C.-W. Chu, *Phys. Rev. B* **79**, 104504 (2009).

¹¹N. Barišić, Y. Li, X. Zhao, Y.-C. Cho, G. Chabot-Couture, G. Yu, and M. Greven, *Phys. Rev. B* **78**, 054518 (2008).

¹²W. Z. Hu, J. Dong, G. Li, Z. Li, P. Zheng, G. F. Chen, J. L. Luo, and N. L. Wang, *Phys. Rev. Lett.* **101**, 257005 (2008).

¹³M. Nakajima *et al.*, *Physica C* (to be published).

¹⁴D. Wu *et al.*, *Phys. Rev. B* **79**, 155103 (2009).

¹⁵G. Li, W. Z. Hu, J. Dong, Z. Li, P. Zheng, G. F. Chen, J. L. Luo, and N. L. Wang, *Phys. Rev. Lett.* **101**, 107004 (2008).

¹⁶Z. G. Chen, G. Xu, W. Z. Hu, X. D. Zhang, P. Zheng, G. F. Chen, J. L. Luo, Z. Fang, and N. L. Wang, *Phys. Rev. B* **80**, 094506 (2009).

¹⁷J. Yang, D. Huvonen, U. Nagel, T. Rõõm, N. Ni, P. C. Canfield, S. L. Budko, J. P. Carbotte, and T. Timusk, *Phys. Rev. Lett.* **102**, 187003 (2009).

¹⁸W. Z. Hu, Q. M. Zhang, and N. L. Wang, *Physica C* **469**, 545 (2009).

¹⁹B. Gorshunov *et al.*, *Phys. Rev. B* **81**, 060509(R) (2010).

²⁰M. Dressel and G. Grüner, *Electrodynamics of Solids* (Cambridge University Press, Cambridge, 2002).

²¹Other decompositions of the optical conductivity than suggested here might be tempting, too. For example, the next simplest one is to fit the low-frequency conductivity by a Drude and a Lorentzian terms. However, there is not really any physical meaning of the Lorentzian, and furthermore its position, width, and amplitude strongly change with temperature which is highly anomalous.

²²D. V. Evtushinsky *et al.*, *New J. Phys.* **11**, 055069 (2009); V. B. Zabolotnyy *et al.*, *Nature (London)* **457**, 569 (2009).

²³F. Rullier-Albenque, D. Colson, A. Forget, and H. Alloul, *Phys. Rev. Lett.* **103**, 057001 (2009).

²⁴A. S. Sefat, M. A. McGuire, B. C. Sales, R. Jin, J. Y. Howe, and D. Mandrus, *Phys. Rev. B* **77**, 174503 (2008).

²⁵S. Suzuki, S. Miyasaka, S. Tajima, T. Kida, and M. Hagiwara, *J. Phys. Soc. Jpn.* **78**, 114712 (2009).

²⁶S. Kasahara *et al.*, arXiv:0905.4427 (unpublished).

²⁷C. C. Homes *et al.*, *Nature (London)* **430**, 539 (2004).

²⁸D. Wu, N. Barišić, N. Driehko, P. Kallina, A. Faridian, B. Gorshunov, M. Dressel, L. J. Li, X. Lin, G. H. Cao, Z. A. Xu, *Physica C* (to be published).

²⁹D. Mattis and J. Bardeen, *Phys. Rev.* **111**, 412 (1958).

³⁰R. Khasanov *et al.*, *Phys. Rev. Lett.* **102**, 187005 (2009).

³¹I. I. Mazin, D. J. Singh, M. D. Johannes, and M. H. Du, *Phys. Rev. Lett.* **101**, 057003 (2008); I. I. Mazin and J. Schmalian, *Physica C* **469**, 614 (2009).

³²The single-gap model significantly deviates from the data in the range of high accuracy between 100 and 300 cm^{-1} because the incoherent σ_B has a large width. The hatched area in Fig. 4(b) indicates the superior description by the two-gap BCS model; it does not imply an unambiguous proof of its size. The experimental results for $(\text{Fe}_{0.95}\text{Ni}_{0.05})_2\text{As}_2$ are qualitatively identical but with a lower value $2\Delta_0^{(1)}=35 \text{ cm}^{-1}$ in the narrow Drude term. The small gaps fall below the range in which reliable data could be acquired.

³³A. B. Kuzmenko, *Physica C* **456**, 63 (2007) and references therein.